

Quantitative Analysis of α -Synuclein Solubility in Living Cells Using Split GFP Complementation

Ahmed Kothawala¹, Kiri Kilpatrick¹, Jose Andres Novoa¹, Laura Segatori^{1,2,3*}

1 Department of Chemical and Biomolecular Engineering, Rice University, Houston, Texas, United States of America, **2** Department of Biochemistry and Cell Biology, Rice University, Houston, Texas, United States of America, **3** Department of Bioengineering, Rice University, Houston, Texas, United States of America

Abstract

Presently incurable, Parkinson's disease (PD) is the most common neurodegenerative movement disorder and affects 1% of the population over 60 years of age. The hallmarks of PD pathogenesis are the loss of dopaminergic neurons in the *substantia nigra pars compacta*, and the occurrence of proteinaceous cytoplasmic inclusions (Lewy bodies) in surviving neurons. Lewy bodies are mainly composed of the pre-synaptic protein alpha-synuclein (α syn), an intrinsically unstructured, misfolding-prone protein with high propensity to aggregate. Quantifying the pool of soluble α syn and monitoring α syn aggregation in living cells is fundamental to study the molecular mechanisms of α syn-induced cytotoxicity and develop therapeutic strategies to prevent α syn aggregation. In this study, we report the use of a split GFP complementation assay to quantify α syn solubility. Particularly, we investigated a series of naturally occurring and rationally designed α syn variants and showed that this method can be used to study how α syn sequence specificity affects its solubility. Furthermore, we demonstrated the utility of this assay to explore the influence of the cellular folding network on α syn solubility. The results presented underscore the utility of the split GFP assay to quantify α syn solubility in living cells.

Citation: Kothawala A, Kilpatrick K, Novoa JA, Segatori L (2012) Quantitative Analysis of α -Synuclein Solubility in Living Cells Using Split GFP Complementation. PLoS ONE 7(8): e43505. doi:10.1371/journal.pone.0043505

Editor: Salvador Ventura, Universitat Autònoma de Barcelona, Spain

Received January 6, 2012; **Accepted** July 24, 2012; **Published** August 22, 2012

Copyright: © 2012 Kothawala et al. This is an open-access article distributed under the terms of the Creative Commons Attribution License, which permits unrestricted use, distribution, and reproduction in any medium, provided the original author and source are credited.

Funding: These authors have no support or funding to report.

Competing Interests: The authors have declared that no competing interests exist.

* E-mail: segatori@rice.edu

Introduction

Parkinson's disease (PD) is the most prevalent neurodegenerative movement disorder, affecting 1% of the world's population over the age of 60 years [1]. The hallmarks of PD pathogenesis are the loss of dopaminergic neurons in the *substantia nigra pars compacta* and the occurrence of cytoplasmic inclusions called Lewy bodies (LB) in surviving dopaminergic neurons [2]. *Post mortem* analyses revealed that the main component of LB is the pre-synaptic protein alpha-synuclein (α syn) and of trace amounts of ubiquitin and molecular chaperones [3], suggesting that they result from the aberrant accumulation and aggregation of misfolded, undegraded α syn. Duplications or triplications of the α syn locus [4,5], as well as mutations in α syn-encoding gene - A53T, A30P & E46K – lead to increased aggregation and have been linked to familial cases of PD [6–10]. Overexpression of α syn results in the formation of inclusion bodies, cytotoxicity and cell death in animal models and cell cultures [11–13]. Misfolding and aggregation of α syn has been associated with impairment of proteasomal degradation, another common trait of PD pathogenesis [14–16]. In summary, aberrant accumulation of misfolded α syn plays a key role in development of PD pathogenesis. Therefore, monitoring α syn aggregation in living cells in a quantitative fashion is important to study the molecular mechanisms associated with α syn-induced cytotoxicity and develop therapeutic strategies for the treatment of PD.

A number of α syn variants containing mutations that alter the protein's rate of aggregation have been characterized [6–9]. Among mutations linked to familial cases of PD, the A53T α syn variant was shown to aggregate at a much faster rate than wt α syn

in cell cultures and *in vitro* [9,10,17]. C-terminal truncations have also been reported to aggregate at higher rates than wt α syn [18–20], demonstrating that the proline-rich C-terminal region plays a fundamental role in limiting α syn misfolding and aggregation [18–22]. A recent study demonstrated that a truncation variant of α syn consisting of amino acids 1–123 (α syn123) readily formed aggregates *in vitro* [19]. Interestingly, it was also shown that truncated α syn accumulates in LB [23], suggesting that lower molecular weight truncated α syn species may have a role in PD pathology. Recently, in an effort to decipher the determinants of α syn aggregation, a rationally designed mutant containing three proline substitutions (TP α syn, containing substitutions A30P, A56P and A76P) was also constructed and demonstrated to resist aggregation *in vitro* [24]. Its solubility in cell cultures, however, is not known.

A number of methods to study α syn aggregation *in vitro* have been reported and include microscopy [21], size-exclusion chromatography [25], and NMR spectroscopy [26]. These techniques rely on the use of purified proteins for analysis. Hence, they preclude the study of α syn aggregation in living cells, which is necessary to decipher the pathogenic mechanisms that lead to increased levels of misfolded and aggregated α syn and to identify gene targets for therapy.

Microscopy based techniques have been used to monitor protein aggregation in living cells [27,28]. Particularly, α syn aggregation can be detected using α syn-specific antibodies [11,29] or by overexpressing α syn variants fused to fluorescent reporters such as GFP [17,30,31]. The main limitation of using GFP fusions as aggregation reporters is that aggregation events that occur after

the formation of the GFP chromophore do not alter fluorescence emission, leading to detection of GFP fluorescence irrespective of α syn aggregation state. To overcome this limitation, techniques that rely on fluorescence complementation have been developed. Particularly, α syn was fused to non-fluorescent complementary GFP fragments and the resulting fusion molecules were co-expressed in mammalian cells. α syn self-association causes close proximity of the two GFP fragments and results in bimolecular fluorescence complementation (BiFC). Hence, the intensity of the fluorescence signal is a measurement of α syn self-association [32–34]. Fluorescence energy resonance transfer (FRET) has also been used to quantify α syn aggregation by fusing two fluorophores to the N- and C-termini of α syn [35]. BiFC and FRET, however, suffer from inherent limitations. Fusion of α syn to highly stable chromophores or to large protein fragments can perturb α syn folding and alter its misfolding-propensity. In addition, these techniques are not optimal to measure protein self-association because they fail to detect homotypic interactions.

In this study, we developed an expression system that allows detecting and quantifying soluble α syn in living cells. We adapted a previously reported split GFP molecule specifically engineered to study protein solubility [36]. This GFP variant is cleaved into two unequal size fragments, a 15-amino acid “sensor” fragment and a large “detector” fragment, that spontaneously complement upon chemical interaction, giving rise to a fluorescence signal [36]. α syn was fused to the sensor fragment, which has minimal effect on the folding and solubility of its fusion partners and can therefore be used as a sensor of α syn solubility. The resulting α syn fusion protein was co-expressed with the large detector fragment in cell cultures. Fluorescent complementation is directly proportional to α syn solubility as it occurs only if the sensor fragment escapes aggregation and is accessible to the detector fragment. The fluorescence of cells expressing wild type α syn was compared to that of cells expressing α syn variants with different aggregation properties: A53T α syn, a C-terminal truncation variant (α syn123), and a rationally designed triple proline mutant (A30P, A56P and A76P) with low propensity to aggregate (TP α syn). Cell fluorescence was also evaluated upon inhibition of proteasomal degradation and was observed to correlate with α syn solubility as predicted from *in vitro* studies. Our results indicate that this method provides a robust platform to quantify α syn solubility in living cells and can be used to study α syn sequence specificity and to monitor the influence of the cell folding network on α syn aggregation.

Results

Quantification of α syn Solubility using the α syn-split GFP Assay

To study α syn solubility in living cells we adapted a previously reported assay based on split GFP complementation [36]. In this assay, GFP is split into two moieties, GFP_{1–10}, the bulk of the β -barrel (detector fragment), and GFP₁₁, a 15-amino acid β -sheet (sensor fragment). GFP fragment complementation was shown to be inversely proportional to aggregation by comparing sequential expression and co-expression of GFP₁₁-tagged proteins and GFP_{1–10} [36]. The small GFP₁₁ tag was previously shown not to affect the folding of the fusion protein [36,37] and was therefore fused to the C-terminal of α syn in this study. The large GFP_{1–10} fragment was co-expressed with α syn-GFP₁₁ in the cytoplasm of mammalian cells. We hypothesized that if α syn is maintained in a soluble state, the GFP₁₁ tag is exposed to the solvent and can complement with GFP_{1–10}, giving rise to a fluorescence signal. On the other hand, α syn aggregation would preclude accessibility of GFP₁₁ to

GFP_{1–10}, thus preventing fluorescence complementation. Hence, GFP fluorescence is expected to be proportional to α syn solubility.

HeLa cells were transfected for the expression of α syn-GFP₁₁ and GFP_{1–10} and GFP fluorescence was evaluated by flow cytometry and fluorescence microscopy (Figure 1). As expected, cells expressing only GFP_{1–10} did not display detectable fluorescent signal (Figure 1A), whereas cells co-expressing α syn-GFP₁₁ and GFP_{1–10} exhibited GFP fluorescence when tested 18 hrs post transfection (Figure 1B). Fluorescence microscopy validated these results (Figure 1, inset), confirming that cell fluorescence is due to GFP fragment complementation. To ensure that the intensity of the fluorescence signal is not limited by the amount of GFP_{1–10} available for complementation with GFP₁₁ and is therefore an accurate measurement of the concentration of soluble α syn, a series of experiments were conducted in which increasing concentrations of plasmid encoding for GFP_{1–10} were used in the transfection procedure. A GFP_{1–10} to GFP₁₁ ratio of 2:1 was sufficient to ensure that fluorescent complementation is not limited by the concentration of GFP_{1–10} but rather depends on the amount of soluble α syn-GFP₁₁ (data not shown), in agreement with previously published work [36,37]. This ratio of plasmid concentrations was used for all subsequent experiments.

Next, we compared wild type α syn to three α syn variants - A53T α syn, TP α syn and a C-terminal truncation mutant consisting of amino acids 1–123 (α syn123). A53T α syn was shown to aggregate faster than wild type α syn in cells and *in vitro* [9,10,17]. The truncated α syn123 has a shortened proline rich C terminal region, making it prone to aggregation in *in vitro* studies [18–20]. TP α syn contains three proline substitutions (A30P, A56P and A76P) that disrupt the protein’s ability to form aggregates *in vitro*, therefore preventing the formation of fibrils even after two weeks of incubation [24]. The solubility and aggregation propensity of TP α syn in living cells, however, is not known. The mutations were introduced in the α syn-GFP₁₁ encoding gene. HeLa cells were transfected with three plasmid encoding the α syn-GFP₁₁ variants, GFP_{1–10}, and mCherry, a highly photostable red fluorescent protein mutant [38] (a gracious gift from Dr. Jonathan Silberg, Rice University), used here as a transfection control. Cells were cultured for 18 hrs and GFP fluorescence measured by flow cytometry. Cells expressing TP α syn exhibited 50% higher fluorescence than cells expressing wild type α syn, whereas, GFP fluorescence was 25% lower in cells expressing A53T and α syn123 (Figure 2A). Results obtained using HeLa cells suggest that the α syn-split GFP assay can be used to quantify α syn solubility in living cells. To validate the use of the α syn-split GFP assay in a cell type more relevant to study the phenotype associated with PD cellular pathogenesis, these experiments were repeated using neuroglioma (H4) cells. As shown in Figure 2B, H4 cells expressing A53T α syn and α syn123 exhibited significantly lower fluorescence than wild type α syn, while GFP fluorescence was significantly higher in H4 cells transfected with TP α syn, confirming the results obtained in HeLa cells.

Fluorescence microscopy images of HeLa cells expressing the α syn-split GFP system are reported in Figure 2C–D and include detection of GFP fluorescence (left column) and detection of mCherry fluorescence (right column). GFP fluorescence was observed to decrease in cells expressing A53T α syn and α syn123 and to increase in cells expressing TP α syn, confirming results obtained with flow cytometry. The intensity of mCherry fluorescence, however, did not change in cells expressing different α syn variants, demonstrating that the differences in GFP fluorescence complementation detected are not due to differences in transfection or expression efficiency, but are rather due to GFP fluorescence complementation. These differences in GFP fluores-

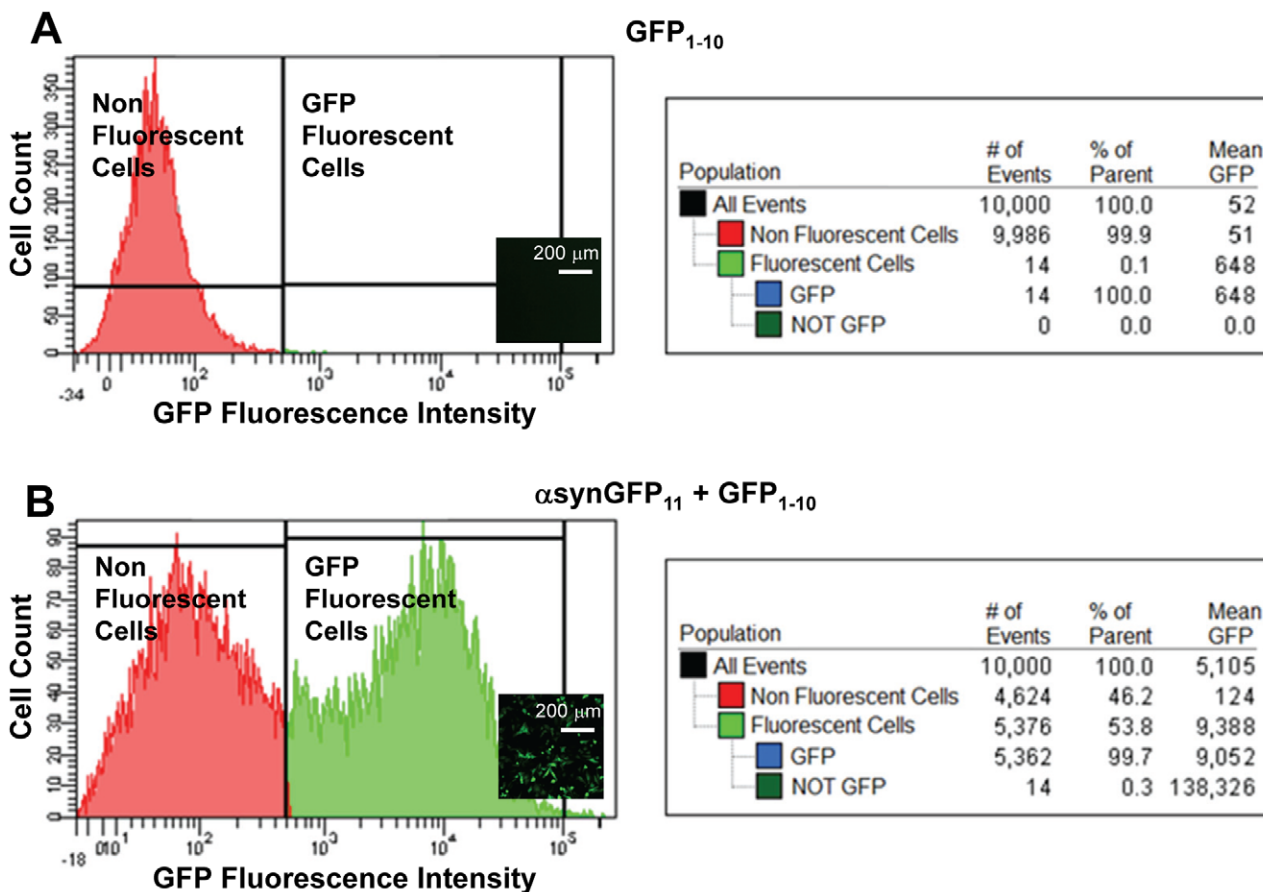


Figure 1. The α -syn-split GFP system enables quantification of soluble α -syn in HeLa cells. HeLa cells were transfected with α -syn-GFP₁₁ and GFP₁₋₁₀. Fluorescence was measured with a flow cytometer and live cells were imaged using fluorescence microscopy. (A) Representative fluorescence histogram (left panel) and data analysis (right panel) of cells expressing GFP₁₋₁₀ only. Over 99% of the cell population does not display fluorescence. A representative image of live cells is reported in the figure inset. (B) Fluorescence histogram (left panel) and data analysis (right panel) of cells co-expressing α -syn-GFP₁₁ and GFP₁₋₁₀. Over 50% of the cell population display GFP fluorescence. A representative fluorescence microscopy image is reported in the figure inset. Scale bars represent 200 μm .

doi:10.1371/journal.pone.0043505.g001

cence complementation were equally observed upon visualization of the whole cell population (Figure 2C) as well as in individual cells (Figure 2D), confirming the results obtained from flow cytometry. In summary, these results demonstrate that A53T α -syn and α -syn123 have a higher propensity to form aggregates and, therefore, lead to lower fluorescence complementation than wt and TP α -syn.

Inhibition of Proteasomal Degradation Lowers α -syn Solubility and Prevents GFP Fluorescence Complementation

Our results demonstrate that the α -syn-split GFP assay is a viable tool to study α -syn aggregation. This assay can be used to study the aggregation of naturally occurring α -syn variants and to predict the aggregation of rationally designed mutants such as TP α -syn. To further characterize the TP α -syn mutant, we tested its solubility in HeLa cells under cell culturing conditions that are expected to alter the solubility of misfolded, aggregation-prone proteins. To this end, we induced chemical inhibition of proteasomal degradation and investigated its effect on fluorescence complementation. Inhibition of the proteasome causes aberrant accumulation of misfolded proteins and formation of insoluble aggregates [39,40]. Lactacystin is a highly selective proteasome inhibitor [41] that can

easily penetrate the cell membrane and irreversibly block multiple hydrolytic activities in the proteasome [42]. HeLa cells expressing GFP₁₋₁₀ and either α -syn-GFP₁₁ or TP α -syn-GFP₁₁ were treated with a range of concentrations of lactacystin for 24 hrs and GFP fluorescence was measured by flow cytometry. As shown in Figure 3A, cells expressing TP α -syn exhibited 10% and 21% higher fluorescence than cells expressing wild type α -syn after 12 and 24 hrs of incubation, respectively. Upon treatment with lactacystin, we observed a decrease in GFP fluorescence in a concentration dependent manner. Specifically, cells expressing α -syn wild type displayed 68% fluorescence of untreated cells upon treatment with 5 μM lactacystin and cells expressing TP α -syn displayed 70% fluorescence under the same conditions (Figure 3B). These results suggest that proteasomal inhibition, by causing an increase in α -syn aggregation, results in lowered GFP fluorescence complementation. Thus, this assay can be used to monitor the influence of the folding and degradation machinery on α -syn solubility. It should be noted that even though lactacystin treatment caused similar changes in fluorescence in cells expressing wild type α -syn and TP α -syn relative to untreated cells, the absolute fluorescence of cells expressing TP α -syn was significantly higher than that of cells expressing α -syn wild type (Figure S1), as reported before (Figure 2 & 3A).

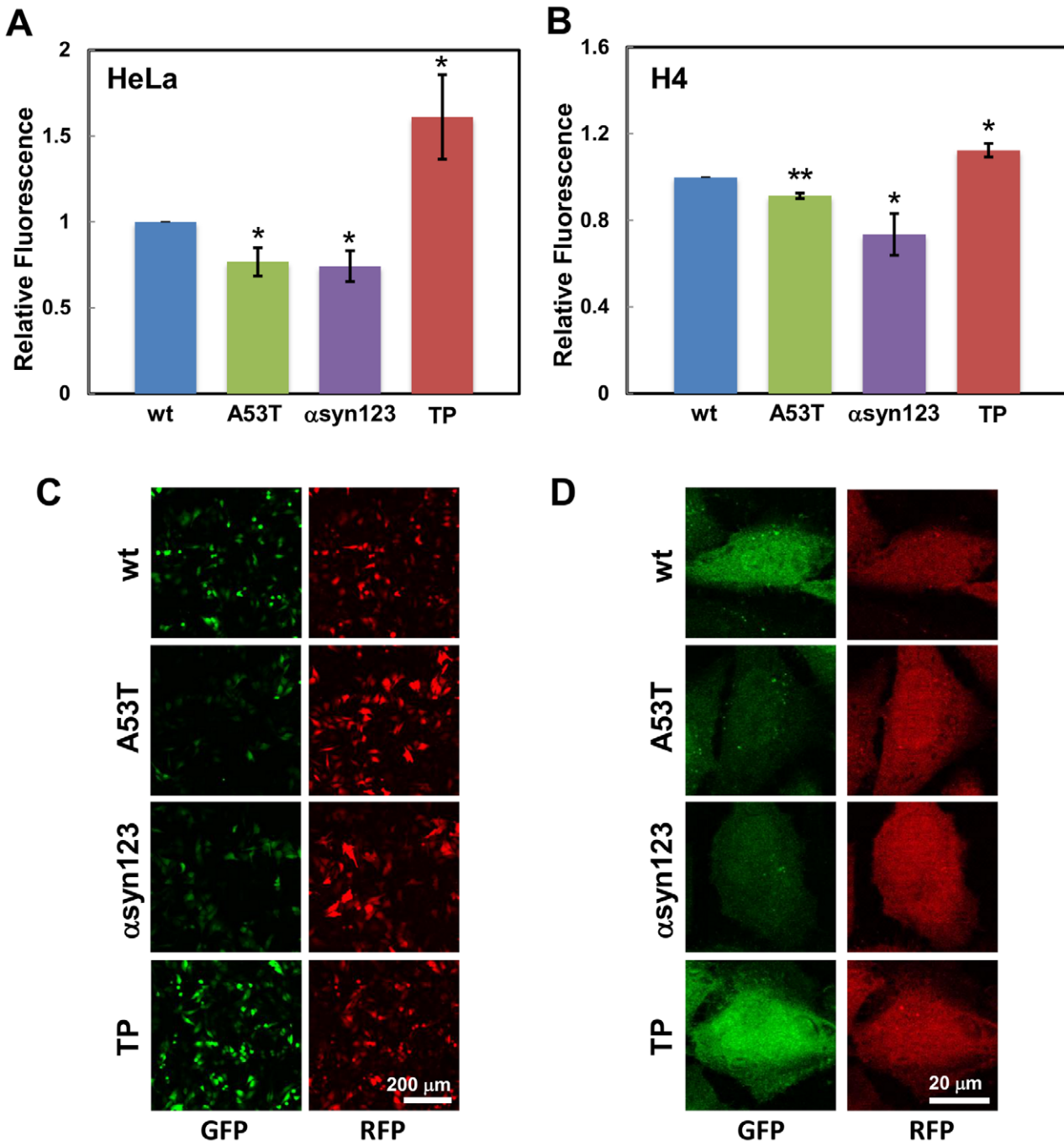


Figure 2. Mutations in α syn gene sequence affect protein solubility. The fluorescence of cells expressing the α syn-split GFP system was measured by flow cytometry and fluorescence microscopy. **(A)** Quantitative analysis of GFP fluorescence of HeLa cells expressing α syn-GFP₁₁+GFP₁₋₁₀ (blue), A53T α syn-GFP₁₁+GFP₁₋₁₀ (green), α syn123-GFP₁₁+GFP₁₋₁₀ (purple) and TP α syn-GFP₁₁+GFP₁₋₁₀ (red). **(B)** Quantitative analysis of GFP fluorescence of H4 cells expressing α syn-GFP₁₁ (blue), A53T α syn-GFP₁₁+GFP₁₋₁₀ (green), α syn123-GFP₁₁+GFP₁₋₁₀ (purple) and TP α syn-GFP₁₁+GFP₁₋₁₀ (red). Fluorescence measurements were normalized to fluorescence of cells expressing wild type α syn-GFP₁₁. * p <0.05; ** p <0.005. Data points are reported as mean \pm S.E.M. (n=3). **(C-D)** Representative fluorescence microscopy images of HeLa cells expressing α syn-GFP₁₁+GFP₁₋₁₀ (blue, first row), A53T α syn-GFP₁₁+GFP₁₋₁₀ (green, second row), α syn123-GFP₁₁+GFP₁₋₁₀ (purple, third row) and TP α syn-GFP₁₁+GFP₁₋₁₀ (red, fourth row) at 20X (C) and 100X (D) magnification. GFP fluorescence is shown in the left column and mCherry fluorescence is shown in the right column. Scale bar represents 200 μ m (C) and 20 μ m (D).

doi:10.1371/journal.pone.0043505.g002

In order to confirm that the loss of GFP fluorescence observed upon lactacystin treatment is due to increase in α syn aggregation, α syn solubility was investigated by Western blot. HeLa cells expressing α syn-GFP₁₁ were incubated with lactacystin (5 μ M) for

24 hrs. The soluble protein fraction was collected and analyzed using an α syn-specific antibody. Lactacystin-induced proteasome inhibition was observed to result in approximately 25% decrease in soluble α syn (Figure 3C and 3D). This data indicates that the

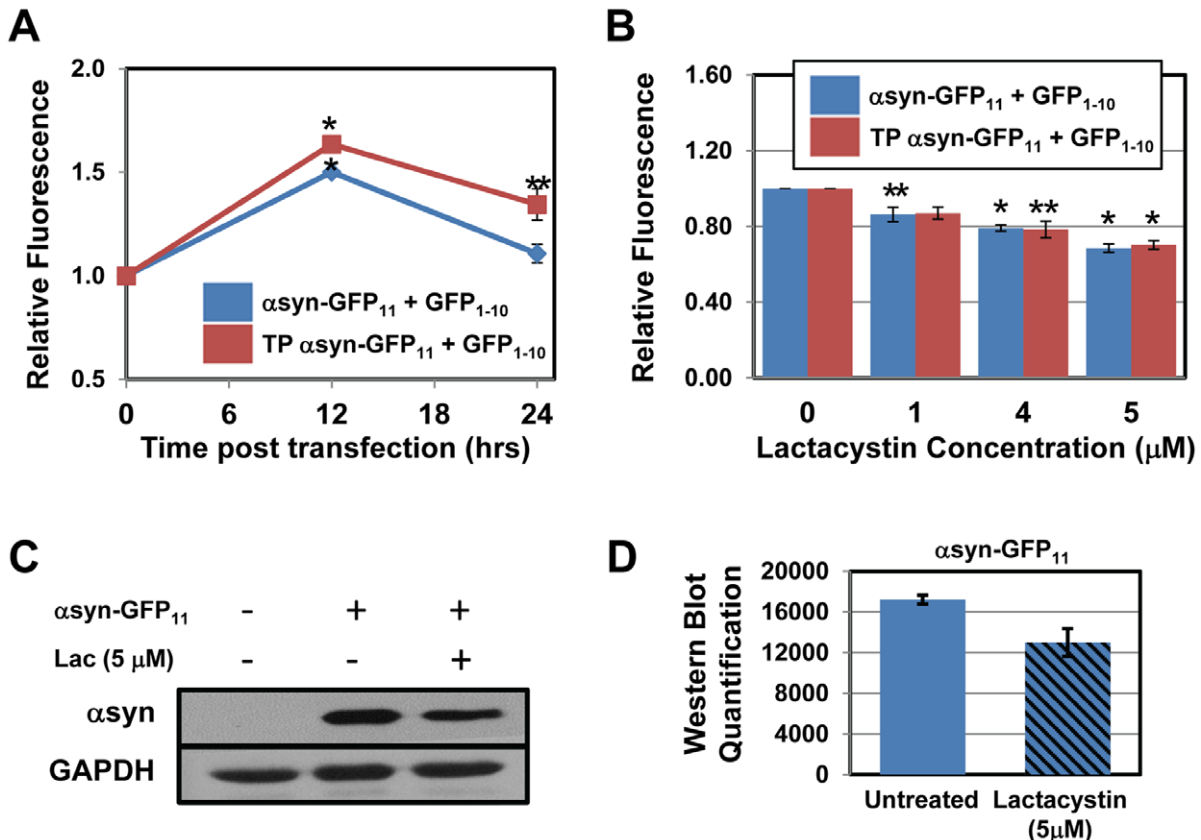


Figure 3. Inhibition of proteasomal degradation lowers α syn solubility. (A) Quantitative analysis of GFP fluorescence of cells expressing α syn-GFP₁₁ + GFP₁₋₁₀ (blue) and TP α syn-GFP₁₁ + GFP₁₋₁₀ (red). Relative fluorescence was calculated by normalizing the fluorescence of cells 12 and 24 hrs post transfection to the fluorescence measured at 0 hr. *p<0.005; **p<0.05. (B) Relative fluorescence of cells expressing α syn-GFP₁₁ and GFP₁₋₁₀ (blue) and TP α syn-GFP₁₁ + GFP₁₋₁₀ (red), 24 hrs post transfection. Cells were incubated for 24 hrs with increasing concentrations of lactacystin (0–5 μ M). Relative fluorescence was evaluated by normalizing the fluorescence of treated cells to the fluorescence of untreated cells. *p<0.01, **p<0.05. Data points are reported as mean \pm S.E.M. (n=3) (C) Representative western blot of cells expressing α syn-GFP₁₁, treated with lactacystin (5 μ M) for 24 hrs, using α syn-specific antibody. (D) Western blots band quantification of cells expressing α syn-GFP₁₁. Bands were quantified by NIH ImageJ analysis software. GAPDH was used as loading control.

doi:10.1371/journal.pone.0043505.g003

decrease in fluorescence complementation due to lactacystin treatment can be attributed to a decrease in soluble α syn-GFP₁₁.

Fluorescence Complementation Inversely Correlates with the Formation of Cellular Aggregates

To examine the correlation between fluorescence complementation and α syn aggregation, we evaluated the formation of aggregates using immunofluorescence microscopy. Cells were cultured under conditions that gave rise to maximal change in GFP complementation and analyzed by immunofluorescence microscopy. Specifically, HeLa cells were transfected for the expression of GFP₁₋₁₀ and either α syn-GFP₁₁ or TP α syn-GFP₁₁ and treated with lactacystin (5 μ M) for 24 hrs. α syn accumulation into cellular aggregates was detected using an antibody specific for α syn (Figure 4, column 1, blue) and the ProteoStat® dye (Figure 4, column 2, red), a 488-nm excitable red fluorescent molecule that specifically interacts with denatured proteins within aggresomes [43]. Images showing co-localization of α syn and the aggregate-specific dye were analyzed with NIH ImageJ software to obtain heatmaps (Figure 4, column 3). To quantify the aggregation of α syn, co-localization events were counted and averaged over three independent experiments. The extent of co-localization was evaluated by analyzing the image heatmaps based on the color

scale reported in Table 1 as described in the Materials and Methods. Our analysis revealed that the degree of α syn aggregation induced by lactacystin treatment depends on α syn sequence. Specifically, cells expressing α syn-GFP₁₁ display a 3-fold increase in α syn aggregation upon treatment with lactacystin, while cells expressing TP α syn-GFP₁₁ exhibit only a 1.5-fold increase (Table 1, high aggregation). The extent of aggregation detected from fluorescence microscopy studies (Figure 4) inversely correlates with measurements of cell fluorescence obtained by flow cytometry (Figure 3). We therefore concluded that the decrease in fluorescence complementation observed in cells treated with lactacystin can be attributed to the increase in α syn aggregation caused by inhibition of proteasomal degradation. Furthermore, the higher fluorescence complementation observed in cells expressing TP α syn compared to wild type α syn is a direct result of its lower rate of aggregation.

Discussion

Aggregation of α syn into proteinaceous inclusions [2] has been repeatedly associated with the development of PD pathogenesis [11,44]. Therefore, there is an urgent need to understand the molecular mechanisms underlying α syn misfolding and aggregation in living cells. Currently available methods to study

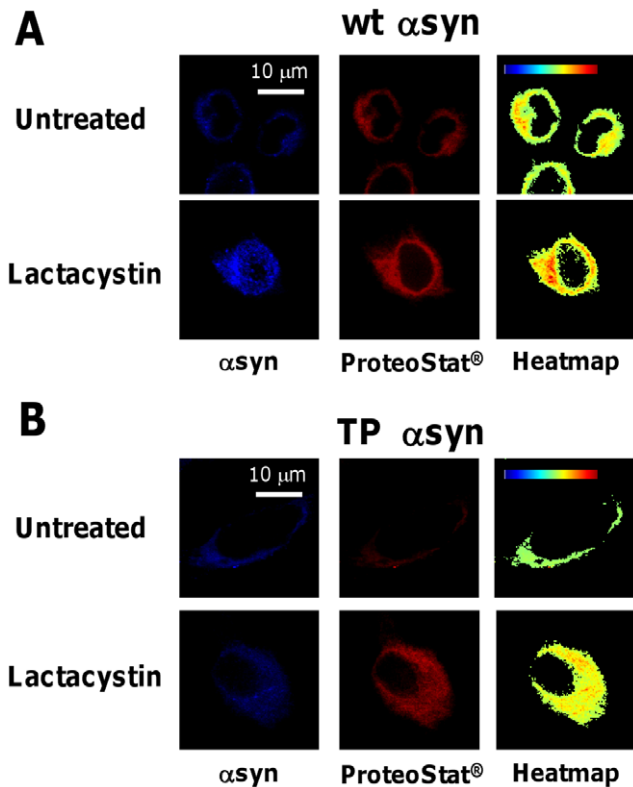


Figure 4. Inhibition of proteasomal degradation enhances αsyn aggregation. Immunofluorescence microscopy of cells expressing (A) αsyn-GFP₁₁ and GFP_{1–10} and (B) TP αsyn-GFP₁₁ and GFP_{1–10}. Cells were treated with lactacystin (5 μM) for 24 hrs. Co-localization intensity of αsyn (blue, column 1) and ProteoStat® dye (red, column 2) is displayed in the form of co-localization heat maps (column 3). Hot colors represent positive co-localization and cold colors represent negative co-localization. Scale bars represent 10 μm.

doi:10.1371/journal.pone.0043505.g004

aggregation in cell cultures, including the use of GFP fusions, BiFC and FRET, present a number of limitations mainly associated with the use of reporter molecules that alter αsyn misfolding and aggregation pathway [32], preclude rapid and high-throughput quantification and, most importantly, do not afford reliable distinction between soluble and insoluble pools of αsyn [45]. In this study, we report the use of a split GFP assay based on the detection of fluorescent complementation [36], previously reported for quantification of protein solubility *in vitro* [36], and in bacterial and mammalian cells [37]. The GFP variant used in this assay is split into a small “sensor” fragment, which was fused to αsyn in this study, and a large “detector” fragment. αsyn aggregation precludes accessibility of the sensor fragment to the

detector fragment for fluorescence complementation. We demonstrated here that the αsyn-split GFP expression system provides a reliable tool to quantify αsyn solubility in living cells.

We investigated the utility of the αsyn-split GFP assay to study the relationship between αsyn sequence and its rate of aggregation in living cells. Mutations in the αsyn-encoding gene have been associated with the development of early onset familial cases of PD [6–8]. αsyn C-terminal truncations were observed to accumulate in LB [20,46,47]. The aggregation properties of naturally occurring and rationally designed αsyn mutants have been extensively characterized *in vitro* [24,48,49]. To evaluate the use of the αsyn-split GFP assay to study how αsyn sequence specificity affects protein aggregation, we tested a rationally designed variant (TP αsyn) known to resist aggregation *in vitro* [24]. We compared the fluorescence of cells expressing TP αsyn to that of cells expressing wild type αsyn, A53T αsyn and a truncated αsyn variant (αsyn123). We observed a significant increase in fluorescence in cells expressing TP αsyn compared to cells expressing wild type αsyn, demonstrating higher solubility of this αsyn variant in cell cultures. On the other hand, cells expressing the A53T mutant and the truncation mutant αsyn123 exhibited significantly lower fluorescence than cells expressing wild type αsyn, suggesting that these variants aggregate at higher rate and that aggregation lowers GFP fragment complementation and fluorescence. These results indicate that the αsyn-split GFP assay can be used to quantify the effect of mutations in αsyn-encoding gene on the protein aggregation propensity in living cells.

We also investigated whether the αsyn-split GFP assay can be used to study the impact of environmental factors that alter the efficiency of the folding quality control system on αsyn solubility. Although the causes of PD are far from understood, studies have shown that changes in the cellular environment such as oxidative stress and inflammation are involved in the progression of the disease [50]. Inducing oxidative stress or inflammation was shown to increase αsyn aggregation and αsyn-induced cytotoxicity [51,52]. Furthermore, the accumulation of αsyn has also been associated with impairment of the proteasome [14–16]. In this study, proteasomal inhibition was chemically induced in cells expressing the αsyn-split GFP system and observed to lower fluorescence complementation, demonstrating that proteasome dysfunction lowers αsyn solubility.

Finally, we showed that the intensity of fluorescence of cells expressing the αsyn-split GFP system is inversely proportional to the extent of αsyn aggregation. Analysis of co-localization between αsyn and an aggregate-specific dye revealed that the increase in fluorescent signal measured correlates with the decrease in aggregate formation. These results demonstrate that the αsyn-split GFP assay can be used to investigate cell treatments that affect protein aggregation and that it will potentially enable molecular screenings for the discovery of compounds that modulate αsyn aggregation.

Table 1. ProteoStat® co-localization assay.

αsyn aggregation	αsyn					TP αsyn						
	Untreated		Lactacystin			Untreated		Lactacystin				
Low ^a	52.0	±	4.5	57.8	±	15.0	33.4	±	6.2	45.7	±	12.0
High ^b	9.8	±	4.6	28.9	±	9.2	7.1	±	4.0	10.8	±	3.0

^aLow co-localization – 35 to 60, yellow pixels.

^bHigh co-localization – 0 to 35, red pixels.

doi:10.1371/journal.pone.0043505.t001

In summary, our results show that the α syn-split GFP assay allows to quantitatively measure the solubility of α syn in living cells. Furthermore, we demonstrated that this assay can be used to study the aggregation properties of α syn mutants in cell cultures and elucidate the effects that modifiers of cellular protein folding have on α syn aggregation.

Methods

Reagents, Cell Lines, and Media

Lactacystin was purchased from Cayman Chemicals. Cell culture media were purchased from Gibco and Invitrogen. Fetal bovine serum (FBS) was purchased from Atlanta Biologicals. JetPrimeTM transfection kit was purchased from Polyplus Transfection. Proteostat[®] Aggresome Detection Kit was purchased from Enzo Life Sciences.

HeLa cells (ATCC) were grown in MEM (GIBCO) supplemented with 10% heat-inactivated FBS and 1% PSQ and maintained at 37°C and 5% CO₂. Human H4 neuroglioma cells (HTB-148, ATCC) were cultured in high glucose DMEM (Invitrogen) supplemented with 10% heat-inactivated FBS, 1% PSQ, 4 mM L-Glutamine, and 1 mM sodium pyruvate, and maintained at 37°C and 5% CO₂. Cell medium was replaced every 3 to 4 days and monolayers of cells were passaged upon reaching about 90% confluence.

Plasmids and Transient Transfections

pCMV-mGFP Cterm S11 Neo Kan and pCMV-mGFP 1–10 Hyg Amp vectors were obtained from Theranostech, Inc. The sequence encoding for GFP_{1–10} was amplified from pCMV-mGFP_{1–10} Hyg Amp by PCR using the primers listed in Table S1 and subcloned into pcDNA4/TO (Invitrogen) using the KpnI and XhoI restriction sites, giving rise to pcDNA4/TO/GFP_{1–10}. The cDNA encoding for α -syn was amplified from pcDNA6.2+ α syn-emGFP plasmid (lab collection) using the primers listed in Table S1 and cloned into the plasmid pCMV-mGFP Cterm S11 Neo Kan using XhoI and AgeI restriction sites, giving rise to pCMV-mGFP/ α syn-GFP₁₁. The A53T substitution carrying mutant α syn was constructed using the QuikChange[®] Site-Directed mutagenesis kit (Stratagene) and KAPA HiFi HotStart PCR kit (Kapa Biosystems) following manufacturers' protocols and using primers listed in Table S1, giving rise to pCMV-mGFP/A53T α syn-GFP₁₁. The gene encoding for the α syn mutant containing A30P, A56P, and A76P substitutions was constructed using the same procedure, using primers listed in Table S1, giving rise to pCMV-mGFP/TP α syn-GFP₁₁. The sequence of the truncated α syn gene was amplified using pCMV-mGFP/ α syn-GFP₁₁ as template and primers listed in Table S1. The PCR product was cloned into the empty pCMV-mGFP Cterm S11 Neo Kan plasmid using XhoI and AgeI restriction sites, giving rise to pCMV-mGFP/ α syn123-GFP₁₁.

Transfections were conducted in 6-well plates. 10⁴ cells were seeded in each well of a 6-well plate and plates were incubated for 24 hrs at 37°C. Transient transfections were performed using the JetPrimeTM DNA transfection kit (Polyplus Transfection) according to the manufacturer's procedures.

GFP Complementation Analyses

HeLa or H4 cells were plated in 6-well plates and incubated for 24 hrs at 37°C. The media was removed and replaced with fresh media containing 0.33 μ g of vectors encoding for wild type α syn, A53T α syn, TP α syn or α syn123 and 0.67 μ g of pcDNA4/TO/GFP_{1–10} per well and transfected as described above. Transfection reactions were incubated for 16 hrs, at which point the media was

replaced again. Cells were then collected and fluorescence was measured using a flow cytometer (FACSCantoTM II, BD Biosciences).

Fluorescence Microscopy Analysis

HeLa cells were seeded on glass coverslips in 6-well plate and incubated for 24 hrs at 37°C. The media was removed and replaced with fresh media containing 0.33 μ g/well of vectors encoding for wild type α syn, A53T, TP α syn or α syn123, 0.67 μ g/well of pcDNA4/TO/GFP_{1–10} and 0.2 μ g/well of plasmid encoding for mCherry. The transfection reactions were incubated for 16 hrs, at which point they were washed with 0.1% Tween-20/PBS and fixed with 4% paraformaldehyde for 30 min. The coverslips were mounted on glass slides for fluorescence microscopy. The slides were imaged using an Olympus IX81 confocal microscope and analyzed using proprietary Fluoview software.

Western Blot Analysis

HeLa cells were plated in 6-well plates and incubated for 24 hrs at 37°C. The media was removed and replaced with fresh MEM media containing 0.5 μ g of pCMV-mGFP/ α syn-GFP₁₁ per well and transfected as described above. Cells were lysed with complete lysis-M buffer (Roche) for 30 min on ice with gentle rocking. The protein concentration was determined by Bradford assay (Pierce), and each sample was diluted to the same protein concentration. Proteins were separated by 12% SDS-polyacrylamide gels and transferred to a nitrocellulose membrane. Membranes were incubated with primary antibodies (mouse anti- α -syn (Sigma-Aldrich) and rabbit anti-GAPDH (Santa Cruz Biotechnology)) and appropriate secondary antibodies (HRP conjugated goat anti-rabbit and goat anti-mouse antibodies (Santa Cruz)). Blots were visualized using Millipore Luminata Forte HRP chemiluminescent substrate (Fisher) and quantified using NIH ImageJ software.

Immunofluorescence and Co-localization Analyses

Cells were seeded on glass coverslips in 6-well plate, transfected, incubated in the presence of small molecules for 24 hrs and fixed with 4% paraformaldehyde for 30 min. Cells were permeabilized with a 0.5% Triton X-100, 0.6% 0.5 M EDTA solution in Assay buffer (Proteostat[®] Aggresome Detection Kit, Enzo) for 30 min on ice, followed by incubation in 8% BSA (blocking buffer) for 1 hr at room temperature. Cells were then incubated for 1 hr with primary antibody (mouse anti- α syn, Sigma-Aldrich), washed with 0.1% Tween-20/PBS, and incubated with secondary antibody (Dylight 649 Goat anti-mouse from KPL). Cells were washed again and incubated with Proteostat[®] dye (Proteostat[®] Aggresome Detection Kit, Enzo) for 30 min in the dark. The coverslips were mounted on glass slides for fluorescent microscopy. The slides were imaged using an Olympus IX81 confocal microscope and analyzed using proprietary Fluoview software.

Co-localization of α syn with the Proteostat[®] dye was evaluated using the ImageJ plugin Co-localization Colormap [53]. Results are reported in the form of co-localization heatmaps where hot colors represent positive co-localization, and cold colors represent negative co-localization. The co-localization heatmaps were analyzed using the ImageJ plugin Threshold Colour, which allows RGB images to be filtered based on the hue, saturation, and brightness of the pixels. Images were filtered to display RGB color hues as follows: high co-localization (RGB hue: 0–35, red pixels) and low co-localization (RGB hue: 36–60, yellow pixels). Pixels falling in the RGB hue range 60–255 were considered negative correlation and not evaluated in this study. For each sample, 85–120 cells were analyzed to count co-localization events.

Statistical Analysis

All data are presented as mean \pm S.E.M. Statistical significance was calculated using a two-tailed Student's t test. Values were considered significantly different when p was <0.05 .

Supporting Information

Figure S1 Effect of inhibition of proteasomal degradation on αsyn solubility and split GFP fluorescence complementation. Representative plot of absolute GFP fluorescence in cells expressing αsyn-GFP₁₁ and GFP₁₋₁₀ (blue) and TP αsyn-GFP₁₁ and GFP₁₋₁₀ (red). Cells were incubated for 24 hrs with increasing concentrations of lactacystin (0–5 μM).

References

1. de Lau LML, Breteler MMB (2006) Epidemiology of Parkinson's disease. *The Lancet Neurology* 5: 525–535.

2. Moore DJ, West AB, Dawson VL, Dawson TM (2005) MOLECULAR PATHOPHYSIOLOGY OF PARKINSON'S DISEASE. *Annual Review of Neuroscience* 28: 57–87.

3. Shultz CW (2006) Lewy bodies. *Proceedings of the National Academy of Sciences of the United States of America* 103: 1661–1668.

4. Chartier-Harlin M-C, Kachergus J, Roumier C, Mouroux V, Douay X, et al. (2004) α-synuclein locus duplication as a cause of familial Parkinson's disease. *The Lancet* 364: 1167–1169.

5. Singleton AB, Farrer M, Johnson J, Singleton A, Hague S, et al. (2003) α-Synuclein Locus Triplication Causes Parkinson's Disease. *Science* 302: 841.

6. Kruger R, Kuhn W, Muller T, Woitalla D, Graeber M, et al. (1998) Ala30Pro mutation in the gene encoding alpha-synuclein in Parkinson's disease. *Nature genetics* 18: 106–108.

7. Polymeropoulos MHLC (1997) Mutation in the alpha-synuclein gene identified in families with Parkinson's disease. *Science* 276: 2045.

8. Zarrazza JJ, Alegre J, Gómez-Esteban JC, Lezcano E, Ros R, et al. (2004) The new mutation, E46K, of α-synuclein causes parkinson and Lewy body dementia. *Annals of Neurology* 55: 164–173.

9. Li J, Uversky VN, Fink AL (2001) Effect of familial Parkinson's disease point mutations A30P and A53T on the structural properties, aggregation, and fibrillation of human alpha-synuclein. *Biochemistry* 40: 11604–11613.

10. Nahrke L, Wood SJ, Steavenson S, Jiang Y, Wu GM, et al. (1999) Both familial Parkinson's disease mutations accelerate alpha-synuclein aggregation. *J Biol Chem* 274: 9843–9846.

11. Rideout HJ, Larsen KE, Sulzer D, Stefanis L (2001) Proteasomal inhibition leads to formation of ubiquitin/α-synuclein-immunoreactive inclusions in PC12 cells. *Journal of Neurochemistry* 78: 899–908.

12. Fleming SM, Salcedo J, Fernagut PO, Rockenstein E, Masliah E, et al. (2004) Early and progressive sensorimotor anomalies in mice overexpressing wild-type human alpha-synuclein. *J Neurosci* 24: 9434–9440.

13. Zhou W, Hurlbert MS, Schaack J, Prasad KN, Freed CR (2000) Overexpression of human alpha-synuclein causes dopamine neuron death in rat primary culture and immortalized mesencephalon-derived cells. *Brain Res* 866: 33–43.

14. Conway KA, Harper JD, Lansbury PT (2000) Fibrils Formed In Vitro from α-Synuclein and Two Mutant Forms Linked to Parkinson's Disease are Typical Amyloid. *Biochemistry* 39: 2552–2563.

15. Lindersson E, Beedholm R, Hojrup P, Moos T, Gai W, et al. (2004) Proteasomal Inhibition by α-Synuclein Filaments and Oligomers. *Journal of Biological Chemistry* 279: 12924–12934.

16. Snyder H, Mensah K, Theisler C, Lee J, Matouschek A, et al. (2003) Aggregated and Monomeric α-Synuclein Bind to the S6' Proteasomal Protein and Inhibit Proteasomal Function. *Journal of Biological Chemistry* 278: 11753–11759.

17. Outeiro TF, Lindquist S (2003) Yeast Cells Provide Insight into Alpha-Synuclein Biology and Pathobiology. *Science* 302: 1772–1775.

18. Serpell LC, Berriman J, Jakes R, Goedert M, Crowther RA (2000) Fiber diffraction of synthetic α-synuclein filaments shows amyloid-like cross-β conformation. *Proceedings of the National Academy of Sciences* 97: 4897–4902.

19. Li W, West N, Colla E, Pletnikova O, Troncoso JC, et al. (2005) Aggregation promoting C-terminal truncation of α-synuclein is a normal cellular process and is enhanced by the familial Parkinson's disease-linked mutations. *Proceedings of the National Academy of Sciences of the United States of America* 102: 2162–2167.

20. Crowther RA, Jakes R, Spillantini MG, Goedert M (1998) Synthetic filaments assembled from C-terminally truncated α-synuclein. *FEBS Letters* 436: 309–312.

21. Goldsbury C, Frey P, Olivieri V, Aebi U, Müller SA (2005) Multiple Assembly Pathways Underlie Amyloid-β Fibril Polymorphisms. *Journal of Molecular Biology* 352: 282–298.

22. Heise H, Hoyer W, Becker S, Andronesi OC, Riedel D, et al. (2005) Molecular-level secondary structure, polymorphism, and dynamics of full-length α-synuclein fibrils studied by solid-state NMR. *Proceedings of the National Academy of Sciences of the United States of America* 102: 15871–15876.

23. Baba M, Nakajo S, Tu PH, Tomita T, Nakaya K, et al. (1998) Aggregation of alpha-synuclein in Lewy bodies of sporadic Parkinson's disease and dementia with Lewy bodies. *Am J Pathol* 152: 879–884.

24. Karpinar DP, Balija MBG, Kugler S, Opazo F, Rezai-Ghaleh N, et al. (2009) Pre-fibrillar [α]-synuclein variants with impaired [β]-structure increase neurotoxicity in Parkinson's disease models. *EMBO J* 28: 3256–3268.

25. Wang W, Perovic I, Chittuluru J, Kaganovich A, Nguyen LTT, et al. (2011) A soluble α-synuclein construct forms a dynamic tetramer. *Proceedings of the National Academy of Sciences* 108: 17797–17802.

26. Etzkorn M, Böckmann A, Baldus M (2011) Kinetic analysis of protein aggregation monitored by real-time 2D solid-state NMR spectroscopy. *Journal of Biomolecular NMR* 49: 121–129.

27. Johnston JA, Ward CL, Kopito RR (1998) Aggresomes: A Cellular Response to Misfolded Proteins. *The Journal of Cell Biology* 143: 1883–1898.

28. Taschenberger G, Garrido M, Tereshchenko Y, Bähr M, Zweckstetter M, et al. (2011) Aggregation of αSynuclein promotes progressive in vivo neurotoxicity in adult rat dopaminergic neurons. *Acta Neuropathologica*: 1–13.

29. Webb JL, Ravikumar B, Atkins J, Skepper JN, Rubinsztein DC (2003) α-Synuclein Is Degraded by Both Autophagy and the Proteasome. *Journal of Biological Chemistry* 278: 25009–25013.

30. McLean PJ, Kawamata H, Hyman BT (2001) α-Synuclein-enhanced green fluorescent protein fusion proteins form proteasome sensitive inclusions in primary neurons. *Neuroscience* 104: 901–912.

31. Schwach G, Tschemmernegg M, Pfragger R, Ingolic E, Schreiner E, et al. (2010) Establishment of stably transfected rat neuronal cell lines expressing alpha-synuclein GFP fusion proteins. *J Mol Neurosci* 41: 80–88.

32. Outeiro TF, Putcha P, Tetzlaff JE, Spoelgen R, Koker M, et al. (2008) Formation of Toxic Oligomeric α-Synuclein Species in Living Cells. *PLoS ONE* 3: e1867.

33. Tetzlaff JE, Putcha P, Outeiro TF, Ivanov A, Berezovska O, et al. (2008) CHIP Targets Toxic α-Synuclein Oligomers for Degradation. *Journal of Biological Chemistry* 283: 17962–17968.

34. Goncalves SA, Matos JE, Outeiro TF (2010) Zooming into protein oligomerization in neurodegeneration using BiFC. *Trends Biochem Sci* 35: 643–651.

35. Klucken J, Outeiro TF, Nguyen P, McLean PJ, Hyman BT (2006) Detection of novel intracellular α-synuclein oligomeric species by fluorescence lifetime imaging. *The FASEB Journal* 20: 2050–2057.

36. Cabantous S, Terwilliger TC, Waldo GS (2005) Protein tagging and detection with engineered self-assembling fragments of green fluorescent protein. *Nat Biotech* 23: 102–107.

37. Chun W, Waldo GS, Johnson GVW (2007) Split GFP complementation assay: a novel approach to quantitatively measure aggregation of tau in situ: effects of GSK3β activation and caspase 3 cleavage. *Journal of Neurochemistry* 103: 2529–2539.

38. Shaner NC, Campbell RE, Steinbach PA, Giepmans BN, Palmer AE, et al. (2004) Improved monomeric red, orange and yellow fluorescent proteins derived from Discosoma sp. red fluorescent protein. *Nat Biotechnol*. United States. 1567–1572.

39. Lecker SH, Goldberg AL, Mitch WE (2006) Protein Degradation by the Ubiquitin-Proteasome Pathway in Normal and Disease States. *Journal of the American Society of Nephrology* 17: 1807–1819.

40. Lehman N (2009) The ubiquitin proteasome system in neuropathology. *Acta Neuropathologica* 118: 329–347.

41. Soldatenkov VA, Dritschilo A (1997) Apoptosis of Ewing's Sarcoma Cells Is Accompanied by Accumulation of Ubiquitinated Proteins. *Cancer Research* 57: 3881–3885.

42. Fenteany G, Standaert R, Lane W, Choi S, Corey E, et al. (1995) Inhibition of proteasome activities and subunit-specific amino-terminal threonine modification by lactacystin. *Science* 268: 726–731.

43. Shen D, Coleman J, Chan E, Nicholson T, Dai L, et al. (2011) Novel Cell- and Tissue-Based Assays for Detecting Misfolded and Aggregated Protein Accumulation Within Aggresomes and Inclusion Bodies. *Cell Biochemistry and Biophysics* 60: 173–185.

(TIF)

Table S1 Primers used to construct GFP₁₋₁₀, wt αsyn-GFP₁₁, A53T αsyn-GFP₁₁, TP αsyn-GFP₁₁, and αsyn123-GFP₁₁.

(DOC)

Author Contributions

Conceived and designed the experiments: AK LS. Performed the experiments: AK KK JAN. Analyzed the data: AK KK. Contributed reagents/materials/analysis tools: AK KK JAN. Wrote the paper: AK KK LS.

44. McNaught KSP, Björklund LM, Belizaire R, Isacson O, Jenner P, et al. (2002) Proteasome inhibition causes nigral degeneration with inclusion bodies in rats. *NeuroReport* 13: 1437–1441.
45. Waldo GS, Standish BM, Berendzen J, Terwilliger TC (1999) Rapid protein-folding assay using green fluorescent protein. *Nat Biotech* 17: 691–695.
46. Du H-N, Tang L, Luo X-Y, Li H-T, Hu J, et al. (2003) A Peptide Motif Consisting of Glycine, Alanine, and Valine Is Required for the Fibrillization and Cytotoxicity of Human α -Synuclein†. *Biochemistry* 42: 8870–8878.
47. Murray IVJ, Giasson BI, Quinn SM, Koppaka V, Axelsen PH, et al. (2003) Role of α -Synuclein Carboxy-Terminus on Fibril Formation in Vitro†. *Biochemistry* 42: 8530–8540.
48. Koo H-J, Lee H-J, Im H (2008) Sequence determinants regulating fibrillation of human α -synuclein. *Biochemical and Biophysical Research Communications* 368: 772–778.
49. Volles MJ, Lansbury PT Jr (2007) Relationships between the Sequence of α -Synuclein and its Membrane Affinity, Fibrillization Propensity, and Yeast Toxicity. *Journal of Molecular Biology* 366: 1510–1522.
50. Hirsch EC, Hunot S (2009) Neuroinflammation in Parkinson's disease: a target for neuroprotection? *The Lancet Neurology* 8: 382–397.
51. Hashimoto M, Hsu IJ, Xia Y, Takeda A, Sisk A, et al. (1999) Oxidative stress induces amyloid-like aggregate formation of NACP/[α]-synuclein in vitro. *NeuroReport* 10: 717–721.
52. Gao H-M, Kotzbauer PT, Uryu K, Leight S, Trojanowski JQ, et al. (2008) Neuroinflammation and Oxidation/Nitration of α -Synuclein Linked to Dopaminergic Neurodegeneration. *The Journal of Neuroscience* 28: 7687–7698.
53. Jaskolski F, Mulle C, Manzoni OJ (2005) An automated method to quantify and visualize colocalized fluorescent signals. *Journal of Neuroscience Methods* 146: 42–49.